

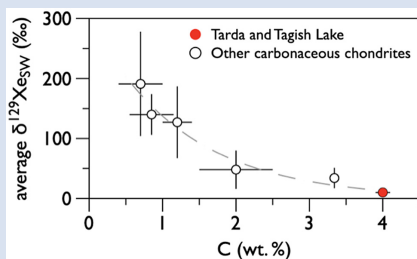
Origin of radiogenic ^{129}Xe variations in carbonaceous chondrites

G. Avice^{1*}, M.M.M. Meier², Y. Marrocchi³



<https://doi.org/10.7185/geochemlet.2228>

Abstract



Carbonaceous chondrites are pristine witnesses of the formation of the solar system. Among them, the carbon-rich Tarda and Tagish Lake meteorites are thought to have sampled very distant regions of the outer circumsolar disk (Hiroi *et al.*, 2001). Here, we show that their noble gas isotopic compositions (especially ^{129}Xe excesses) are similar, implying their formation in comparable environments. Combined with literature data, we show that the radiogenic excesses of ^{129}Xe relative to solar wind in carbonaceous chondrites define anti-correlations with their respective iodine and carbon contents. These trends do not result from the heterogeneous distribution of ^{129}I in the disk but rather evidence a xenon dilution effect; the radiogenic ^{129}Xe excesses being dominated by trapped xenon in the most carbon-rich carbonaceous chondrites. Our data also suggest that both Tarda and Tagish Lake accreted beyond 10 astronomical units, in regions of the disk that were cold enough for CO_2 to condense.

Received 6 April 2022 | Accepted 19 July 2022 | Published 23 August 2022

Introduction

Noble gases trapped in primitive meteorites (chondrites) allow quantification of the physical processes that operated during the evolution of the protoplanetary disk (e.g., Kuga *et al.*, 2015). Although these elements are present in different carriers contained in meteorites (including presolar SiC, diamonds, graphite; Ott, 2014), they are mainly hosted in a phase – referred to as phase Q – whose nature is still poorly characterised (Busemann *et al.*, 2000). Notwithstanding this uncertainty, it has been shown that phase Q dominates the heavy noble gas budget of chondrites and is closely associated with carbonaceous material that survives HF/HCl attack of bulk meteorites (Lewis *et al.*, 1975). Thanks to its extreme sensitivity to oxidation, the xenon isotopic composition of phase Q has been precisely determined, revealing a mass dependent isotopic fractionation relative to solar wind (SW-Xe) in favour of the heavy isotopes relative to the light ones (Wieler *et al.*, 1991; Busemann *et al.*, 2000; Gilmour, 2010). However, the commonly used Xe-Q isotopic composition hinges on the average of measurements of several carbonaceous chondrites (CCs) showing distinct Xe isotopic compositions between and within each group, especially for ^{129}Xe (Busemann *et al.*, 2000). Such ^{129}Xe excesses result from the decay of extinct ^{129}I ($t_{1/2} = 16$ Myr), which was producing radiogenic $^{129}\text{Xe}^*$ during the first ~100 million years of the solar system (Jeffery and Reynolds, 1961). The measurement of xenon isotopes in the coma of comet 67P/Churyumov-Gerasimenko revealed extreme ^{129}Xe enrichment relative to ^{132}Xe and the solar composition (Marty *et al.*, 2017). As this large monoisotopic excess would require unlikely ^{129}I enrichment, it has been interpreted as originating from a specific nucleosynthetic process

producing ^{129}Xe that was sampled by icy bodies formed in the outer solar system (Marty *et al.*, 2017). Interestingly, the carbon-rich primitive chondrites Tagish Lake and Tarda are thought to originate from D-type asteroids (Hiroi *et al.*, 2001; Marrocchi *et al.*, 2021) considered to have formed at large heliocentric distances beyond the current orbit of Saturn, and potentially as far as the Kuiper Belt (*i.e.* 30–50 astronomical units = au; Levison *et al.*, 2009). Here we report the results of a comprehensive study of the isotopic compositions of noble gases contained in Tagish Lake and Tarda to evaluate if material accreted in the outer solar system presents specific signatures. We compare our data to other CCs and discuss the origin of the variable radiogenic ^{129}Xe excesses between and within each CC groups.

Material and Methods

Noble gases were extracted from bulk fragments of Tarda, Tagish Lake and Orgueil meteorites by a laser step-heating method and measured with a noble gas mass spectrometer. Uncertainties on isotope ratios include internal uncertainties, external uncertainties assessed by measurements of standard aliquots, and uncertainties on the blank contribution. Details on the analytical procedure are in the [Supplementary Information](#).

Results of Noble Gas Measurements and Cosmic-ray Exposure Ages

Abundances and isotopic compositions of Ne, Ar, Kr and Xe extracted from bulk Tarda, Tagish Lake and Orgueil samples are reported in [Table S-1](#). Elemental abundances of Ne, Ar,

1. Université Paris Cité, Institut de physique du globe de Paris, CNRS, Paris, F-75005, France
2. Naturmuseum St. Gallen, Rorschacher Strasse 263, St. Gallen, CH-9016, Switzerland
3. Université de Lorraine, CNRS, CRPG, UMR 7358, Vandœuvre-lès-Nancy, F-54500, France

* Corresponding author (email: avice@ipggp.fr)



Kr and Xe in Tarda, Tagish Lake and Orgueil are similar to those reported for other volatile-rich carbonaceous chondrites (Table S-1; Mazor *et al.*, 1970). Most heating steps show a similar $^{20}\text{Ne}/^{132}\text{Xe}$ ratio (average value of 22 ± 4), slightly lower than the range reported for the HL component (50 ± 20 ; Huss and Lewis, 1994). For all samples, $^{36}\text{Ar}/^{132}\text{Xe}$ and $^{84}\text{Kr}/^{132}\text{Xe}$ ratios plot close to the Q component although the first, low temperature, heating steps are systematically plotting toward higher $^{84}\text{Kr}/^{132}\text{Xe}$ ratios, which are compatible with a contribution from weakly bound atmospheric gases (Fig. S-1). For all heating steps, the isotopic composition of neon indicates the presence of abundant trapped neon in the different meteorite samples (Fig. 1). Data points of heating steps of Tarda and Tagish Lake samples plot slightly below a mixing line defined by Ne-HL (Huss and Lewis, 1994) and cosmogenic neon (Supplementary Information). The two first heating steps of Orgueil samples plot on the Ne-Q/cosmogenic mixing line while the high temperature extraction steps show lower $^{21}\text{Ne}/^{22}\text{Ne}$ ratios and plot close to the Ne-Q/Ne-HL mixing line. For argon, $^{38}\text{Ar}/^{36}\text{Ar}$ ratios are compatible with either the atmospheric $^{38}\text{Ar}/^{36}\text{Ar}$ ratio (≈ 0.188 ; Ozima and Podosek, 2002) or the $^{38}\text{Ar}/^{36}\text{Ar}$ ratio of argon in phase Q (≈ 0.187 ; Ott, 2002). However, the $^{40}\text{Ar}/^{36}\text{Ar}$ ratios range from 3 to 43, well below the atmospheric value (≈ 300 , Ozima and Podosek, 2002), but typical for trapped argon contained in carbonaceous chondrites (Krietsch *et al.*, 2021). The isotopic ratios of Kr and Xe are distinct from those of air, as well, and are similar again, to those measured for bulk carbonaceous chondrites (e.g., Krietsch *et al.*, 2021). The first heating steps of Tarda and Tagish Lake samples reveal the presence of weakly bound atmospheric gases (Fig. S-2). For the $^{129}\text{Xe}/^{130}\text{Xe}$ ratio, high temperature heating steps of Tarda and Tagish Lake samples gave reproducible results with an average value of 6.37 ± 0.01 (1σ s.d.). This value is 8.3 ± 3.4 ‰ lower than the $^{129}\text{Xe}/^{130}\text{Xe}$ measured for Q-Xe (Busemann *et al.*, 2000). High temperature heating steps of Orgueil samples reveal the presence of excess radiogenic ^{129}Xe compared to Q-Xe.

The presence of abundant trapped Ne in both Tarda and Tagish Lake prevents us from determining precisely the cosmogenic $^{22}\text{Ne}/^{21}\text{Ne}$ ratio and thus cosmogenic ^{21}Ne production

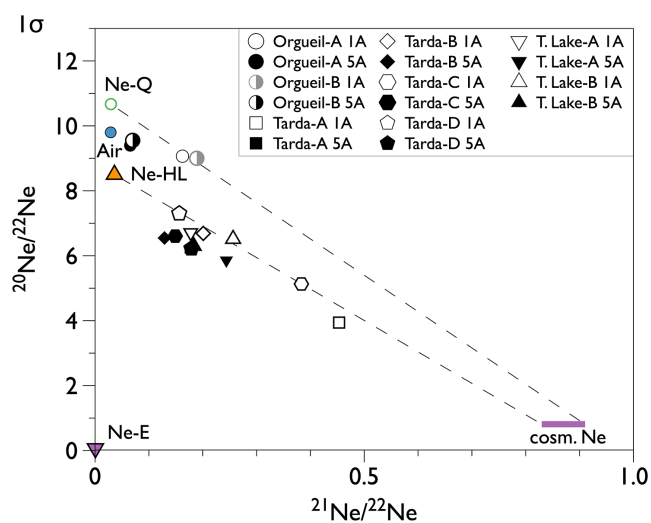


Figure 1 Neon three isotope plot for bulk samples of Tarda, Tagish Lake and Orgueil. The compositions of Ne-Q, Air, Ne-HL, Ne-E and cosmogenic (purple range) are also shown for comparison (see Ott, 2014 and Krietsch *et al.*, 2021 and refs. therein). The two dashed lines represent mixing arrays between Ne-Q and cosmogenic neon and Ne-HL and cosmogenic neon. Error bars (1σ) are smaller than the symbols.

rates (Supplementary Information). Tarda has a cosmic ray exposure (CRE) age within 5–12 Ma, very similar to Tagish Lake (5–8 Ma), while for Orgueil, the possible CRE age ranges from 6 to 11 Ma. The nominal (K-Ar) radiogenic gas retention ages are 2.4–2.7 Ga for Tarda, 2.0–2.8 Ga for Tagish Lake, and 2.2–2.7 Ga for Orgueil.

Discussion

Based on multiple isotopic systems (*i.e.* H, C, N and O), it has recently been proposed that Tarda and Tagish Lake could be genetically related (Marrocchi *et al.*, 2021). This hypothesis can be tested in the light of noble gas measurements reported here. In the three isotope diagram, the neon isotopic compositions of bulk chondrites plot within a space defined by cosmogenic Ne, Ne-Q and a pole with ($^{20}\text{Ne}/^{22}\text{Ne}$) slightly below that of Ne-HL carried by presolar nanodiamonds (Fig. 1; Huss and Lewis, 1994; Krietsch *et al.*, 2021). The latter is likely due to the presence of Ne-E from presolar SiC or graphite (Riebe *et al.*, 2020). The data points from Tarda and Tagish Lake plot on the lower part of this isotopic space with similar Ne isotopic compositions, which are clearly resolved from that of the CI chondrite Orgueil (Fig. 1). Our results show that both Tarda and Tagish Lake have similar bulk Xe spectra and $^{129}\text{Xe}^*$ excesses (Fig. 2), with $\delta^{129}\text{Xe}_{\text{SW}} = 10 \pm 3$ ‰ (Fig. 3a). In addition, both chondrites show similar cosmic-ray exposure and radiogenic retention ages: 5–10 Ma and 2.4–2.7 Ga for Tarda, and 5–8 Ma and 2.0–2.8 Ga for Tagish Lake. Altogether, our results thus reinforce the genetic link between Tarda and Tagish Lake, which share similar isotopic signatures for elements having drastically different geochemical behaviour (Marrocchi *et al.*, 2021).

Xenon in the Jupiter-family comet 67P/Churyumov-Gerasimenko (67P/C-G) presents a ^{129}Xe excess and important, tens of percent $^{134}\text{--}^{136}\text{Xe}$ deficits relative to SW-Xe (Marty *et al.*, 2017). The former has been attributed as resulting from the contribution of parentless ^{129}Xe and the latter of a mixture of two nucleosynthetic processes (*i.e.* s- and r-process; Marty *et al.*, 2017) different from the one measured for most inner solar system material (Avicé *et al.*, 2020). This is however not observed in Orgueil, Tarda and Tagish Lake (Fig. 2) whereas they are generally thought to have formed in the outer solar system, at large heliocentric distances >10 au (Desch *et al.*, 2018; Fujiya *et al.*, 2019; Marrocchi *et al.*, 2021). These meteorites are even showing among the weakest $^{129}\text{Xe}^*$ excesses measured in CCs (Fig. 3a;

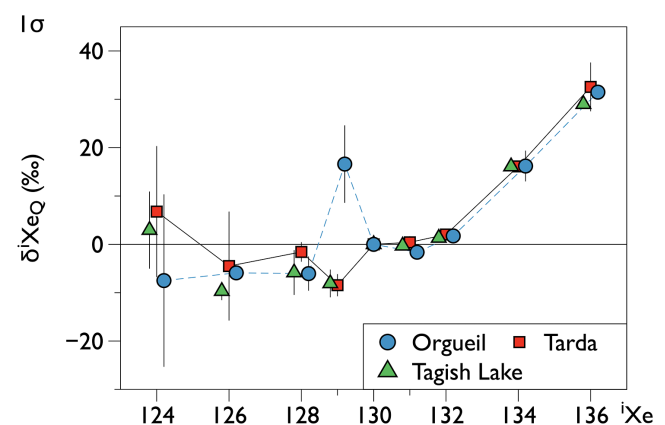


Figure 2 Isotopic composition of total xenon extracted from bulk Tarda, Tagish Lake and Orgueil samples. Isotopic ratios are normalised to Q-Xe (Busemann *et al.*, 2000) and expressed with the delta notation ($\delta^{129}\text{Xe}_Q = ((^{129}\text{Xe}/^{130}\text{Xe})_{\text{sample}} / (^{129}\text{Xe}/^{130}\text{Xe})_Q - 1) \times 1000$). Errors are at 1σ .

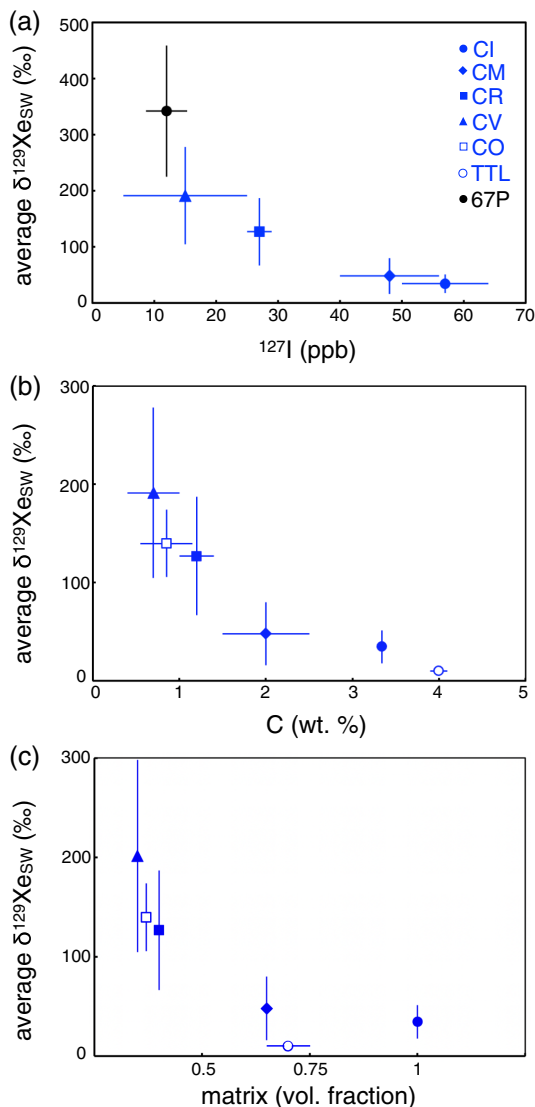


Figure 3 Average $^{129}\text{Xe}^*$ excesses relative to SW-Xe (expressed in δ notation with $\delta^{129}\text{Xe}_{\text{SW}} = \frac{(^{129}\text{Xe}/^{132}\text{Xe})_{\text{bulk}}}{(^{129}\text{Xe}/^{132}\text{Xe})_{\text{SW}}} - 1 \times 1000$) for the different types of chondrites and the comet 67P/C-G (data from Mazor *et al.*, 1970; Marty *et al.*, 2017 and this study). The average $\delta^{129}\text{Xe}_{\text{SW}}$ is plotted as a function of (a) the ^{127}I content (data from Clay *et al.*, 2017), (b) the carbon content (data from Vacher *et al.*, 2020 and Marrocchi *et al.*, 2021), and (c) the matrix abundance (data from Alexander *et al.*, 2018). TTL = Tarda and Tagish Lake.

Mazor *et al.*, 1970). Some rare CMs show similar $^{129}\text{Xe}/^{132}\text{Xe}$ but suffered from significant heating (Alexander *et al.*, 2012; Krietsch *et al.*, 2021). In addition, when combining data from all CCs and the comet 67P (Mazor *et al.*, 1970; Clay *et al.*, 2017; Marty *et al.*, 2017), we observe an anti-correlation of their ^{127}I content and the ^{129}Xe excess (Fig. 3a), regardless of the available iodine dataset used (Fig. S-4). As previously noticed (Mazor *et al.*, 1970; Gilmour *et al.*, 2001), such an inverse correlation could not result from the heterogeneous ^{129}I distribution in the early solar system as the absolute concentrations of radiogenic $^{129}\text{Xe}^*$ vary by only a factor of ~ 4 among CCs, while relative $^{129}\text{Xe}^*$ enrichments differ by a factor of 400.

CCs contains variable amounts of carbon with Tarda, Tagish Lake, CI and CM chondrites showing the highest concentrations (Fig. 3b; Kerridge, 1985; Vacher *et al.*, 2020;

Marrocchi *et al.*, 2021). With the exception of Tarda and Tagish Lake, the carbon content of CCs is directly related to the abundance of fine grained matrix (see Fig. 3 in Alexander *et al.*, 2018). Interestingly, the $^{129}\text{Xe}^*$ excess is also anti-correlated with the bulk C content of CCs (Fig. 3b), thus implying that the (i) ^{129}I carrier was located in the CC matrices, and (ii) variations of $^{129}\text{Xe}^*$ excesses observed in CCs result from a dilution effect by trapped Xe located in phase Q. Such an effect can be summarised as follows: the less carbon, the less phase Q, the less trapped ^{129}Xe , the more the effect of ^{129}I decay is visible (and *vice versa*). This also indicates that the initial Xe budget (and likely that of other noble gases) in CCs is directly controlled by the abundance of matrix (Fig. 3c). Of note, similar $^{129}\text{Xe}^*$ -C anti-correlations are also observed within several CC groups (see Fig. S-5).

Although both Tarda and Tagish Lake are depleted in fine grained matrix relative to CI chondrites (65–80 *vs.* 100 vol. %, Fig. 3c; Alexander *et al.*, 2018), they appear enriched in C (*i.e.* ~ 4 *vs.* 3.3 wt. %, Fig. 3b; Vacher *et al.*, 2020; Marrocchi *et al.*, 2021). This excess has been attributed to the unusual abundance of carbonates in some highly altered lithologies of Tagish Lake (Alexander *et al.*, 2018). However, the bulk C content of Tagish Lake is relatively homogenous (Marrocchi *et al.*, 2021) regardless of the abundance of carbonates (*i.e.* 4.1 ± 0.1 wt. %). In addition, Tarda shows a carbon content similar to Tagish Lake whereas no specific carbonate-rich lithology has been described so far (Marrocchi *et al.*, 2021 and references therein). This thus requires an additional source of carbon for accounting for the diluted $^{129}\text{Xe}^*$ excesses observed in both Tarda and Tagish Lake (Figs. 2, 3a). It has been recently proposed that peculiar carbon isotopic compositions of carbonates in Tagish Lake (*i.e.* $\delta^{13}\text{C} \approx 70$ ‰; Fujiya *et al.*, 2019) cannot be explained without invoking the accretion of large amounts of ^{13}C -rich CO_2 cometary ices. This implies that the parent body of Tagish Lake (and Tarda) formed beyond 10 au, in regions of the protoplanetary disk that were cold enough for CO_2 to condense.

Conclusions

Results obtained in this study demonstrate that Tarda and Tagish Lake, in addition to C, H, N isotope systematics (Marrocchi *et al.*, 2021), present very similar compositions for noble gases. This implies that those meteorites are genetically related and may have sampled similar environments of the accretion disk. A key feature of xenon present in these two meteorites is a very low excess of radiogenic $^{129}\text{Xe}^*$. When compared to literature data of carbonaceous chondrites, these carbon-rich meteorite samples present inverse correlations between $^{129}\text{Xe}^*$ and carbon or iodine content. We interpret these anti-correlations as evidence for a dilution effect of radiogenic $^{129}\text{Xe}^*$ by primordial xenon trapped in organic matter.

Author Contributions

GA and YM designed the study. GA performed the measurements. MM reconstructed the cosmic histories. All authors worked on the data and on the manuscript.

Acknowledgements

Matthieu Gounelle is warmly thanked for fruitful discussions on iodine nucleosynthesis. We acknowledge the financial support of the "Programme National de Planétologie" (PNP). We thank Wataru Fujiya and Henner Busemann for helpful reviews, and Maud Boyet for editorial handling.



Editor: Maud Boyet

Additional Information

Supplementary Information accompanies this letter at <https://www.geochemicalperspectivesletters.org/article2228>.



© 2022 The Authors. This work is distributed under the Creative Commons Attribution Non-Commercial No-Derivatives 4.0

License, which permits unrestricted distribution provided the original author and source are credited. The material may not be adapted (remixed, transformed or built upon) or used for commercial purposes without written permission from the author. Additional information is available at <https://www.geochemicalperspectivesletters.org/copyright-and-permissions>.

Cite this letter as: Avicé, G., Meier, M.M.M, Marrocchi, Y. (2022) Origin of radiogenic ^{129}Xe variations in carbonaceous chondrites. *Geochem. Persp. Let.* 23, 1–4. <https://doi.org/10.7185/geochemlet.2228>

References

- ALEXANDER, C.M.O'D., BOWDEN, R., FOGEL, M.L., HOWARD, K.T., HERD, C.D.K., NITTLER, L.R. (2012) The Provenances of Asteroids, and Their Contributions to the Volatile Inventories of the Terrestrial Planets. *Science* 337, 721–723. <https://doi.org/10.1126/science.1223474>
- ALEXANDER, C.M.O'D., McKEEGAN, K.D., ALTWEGG, K. (2018) Water Reservoirs in Small Planetary Bodies: Meteorites, Asteroids, and Comets. *Space Science Reviews* 214, 47. <https://doi.org/10.1007/s11214-018-0474-9>
- AVICÉ, G., MOREIRA, M., GILMOUR, J.D. (2020) Xenon Isotopes Identify Large-scale Nucleosynthetic Heterogeneities across the Solar System. *The Astrophysical Journal* 889, 68. <https://doi.org/10.3847/1538-4357/ab5f0c>
- BUSEMANN, H., BAUR, H., WIELER, R. (2000) Primordial noble gases in “phase Q” in carbonaceous and ordinary chondrites studied by closed-system stepped etching. *Meteoritics & Planetary Science* 35, 949–973. <https://doi.org/10.1111/j.1945-5100.2000.tb01485.x>
- CLAY, P.L., BURGESS, R., BUSEMANN, H., RUZÍE-HAMILTON, L., JOACHIM, B., DAY, J.M.D., BALLENTINE, C.J. (2017) Halogens in chondritic meteorites and terrestrial accretion. *Nature* 551, 614–618. <https://doi.org/10.1038/nature24625>
- DESCH, S.J., KALYAAN, A., ALEXANDER, C.M.O'D. (2018) The Effect of Jupiter’s Formation on the Distribution of Refractory Elements and Inclusions in Meteorites. *The Astrophysical Journal Supplement Series* 238, 11. <https://doi.org/10.3847/1538-4365/aad95f>
- FUJII, W., HOPPE, P., USHIKUBO, T., FUKUDA, K., LINDGREN, P., LEE, M.R., KOIKE, M., SHIRAI, K., SANO, Y. (2019) Migration of D-type asteroids from the outer Solar System inferred from carbonate in meteorites. *Nature Astronomy* 460, 364. <https://doi.org/10.1038/s41550-019-0801-4>
- GILMOUR, J.D. (2010) “Planetary” noble gas components and the nucleosynthetic history of solar system material. *Geochimica et Cosmochimica Acta* 74, 380–393. <https://doi.org/10.1016/j.gca.2009.09.015>
- GILMOUR, J.D., WHITBY, J.A., TURNER, G. (2001) Negative correlation of iodine-129/iodine-127 and xenon-129/xenon-132: Product of closed-system evolution or evidence of a mixed component. *Meteoritics & Planetary Science* 36, 1283–1286. <https://doi.org/10.1111/j.1945-5100.2001.tb01961.x>
- HIROI, T., ZOLENSKY, M.E., PIETERS, C.M. (2001) The Tagish Lake Meteorite: A Possible Sample from a D-Type Asteroid. *Science* 293, 2234–2236. <https://doi.org/10.1126/science.1063734>
- HUSS, G.R., LEWIS, R.S. (1994) Noble gases in presolar diamonds I: Three distinct components and their implications for diamond origins. *Meteoritics* 29, 791–810. <https://doi.org/10.1111/j.1945-5100.1994.tb01094.x>
- JEFFERY, P.M., REYNOLDS, J.H. (1961) Origin of excess Xe^{129} in stone meteorites. *Journal of Geophysical Research* 66, 3582–3583. <https://doi.org/10.1029/JZ066i010p03582>
- KERRIDGE, J.F. (1985) Carbon, hydrogen and nitrogen in carbonaceous chondrites: Abundances and isotopic compositions in bulk samples. *Geochimica et Cosmochimica Acta* 49, 1707–1714. [https://doi.org/10.1016/0016-7037\(85\)90141-3](https://doi.org/10.1016/0016-7037(85)90141-3)
- KRIETSCH, D., BUSEMANN, H., RIEBE, M.E.I., KING, A.J., ALEXANDER, C.M.O'D., MADEN, C. (2021) Noble gases in CM carbonaceous chondrites: Effect of parent body aqueous and thermal alteration and cosmic ray exposure ages. *Geochimica et Cosmochimica Acta* 310, 240–280. <https://doi.org/10.1016/j.gca.2021.05.050>
- KUGA, M., MARTY, B., MARROCCHI, Y., TISSANDIER, L. (2015) Synthesis of refractory organic matter in the ionized gas phase of the solar nebula. *Proceedings of the National Academy of Sciences* 112, 7129–7134. <https://doi.org/10.1073/pnas.1502796112>
- LEVISON, H.F., BOTKE, W.F., GOUNELLE, M., MORBIDELLI, A., NESVORNÝ, D., TSIGANIS, K. (2009) Contamination of the asteroid belt by primordial trans-Neptunian objects. *Nature* 460, 364–366. <https://doi.org/10.1038/nature08094>
- LEWIS, R.S., SRINIVASAN, B., ANDERS, E. (1975) Host Phase of a Strange Xenon Component in Allende. *Science* 190, 1251–1262.
- MARROCCHI, Y., AVICÉ, G., BARRAT, J.-A. (2021) The Tarda Meteorite: A Window into the Formation of D-type Asteroids. *The Astrophysical Journal Letters* 913, 8. <https://doi.org/10.3847/2041-8213/abfaa3>
- MARTY, B., ALTWEGG, K., BALSIGER, H., BAR-NUN, A., BEKAERT, D.V., BERTHELIER, J.J., BIELER, A., BRIOIS, C., CALMONTE, U., COMBI, M., DE KEYSER, J., FIETHE, B., FUSELIER, S.A., GASC, S., GOMBOSI, T.I., HANSEN, K.C., HÄSSIG, M., JACKEL, A., KOPP, E., KÖRTH, A., LE ROY, L., MALL, U., MOUSIS, O., OWEN, T., REME, H., RUBIN, M., SEMON, T., TZOU, C.Y., WAITE, J.H., WURZ, P. (2017) Xenon isotopes in 67P/Churyumov-Gerasimenko show that comets contributed to Earth’s atmosphere. *Science* 356, 1069–1072. <https://doi.org/10.1126/science.aal3496>
- MAZOR, E., HEYMANN, D., ANDERS, E. (1970) Noble gases in carbonaceous chondrites. *Geochimica et Cosmochimica Acta* 34, 781–824. [https://doi.org/10.1016/0016-7037\(70\)90031-1](https://doi.org/10.1016/0016-7037(70)90031-1)
- OTT, U. (2002) Noble gases in meteorites - Trapped Components. *Reviews in Mineralogy and Geochemistry* 47, 71–100. <https://doi.org/10.2138/rmg.2002.47.3>
- OTT, U. (2014) Planetary and pre-solar noble gases in meteorites. *Chemie der Erde - Geochemistry* 74, 519–544. <https://doi.org/10.1016/j.chemer.2014.01.003>
- OZIMA, M., PODOSEK, F.A. (2002) *Noble Gas Geochemistry*. Cambridge University Press, Cambridge.
- RIEBE, M.E.I., BUSEMANN, H., ALEXANDER, C.M.O'D., NITTLER, L.R., HERD, C.D.K., MADEN, C., WANG, J., WIELER, R. (2020) Effects of aqueous alteration on primordial noble gases and presolar SiC in the carbonaceous chondrite Tagish Lake. *Meteoritics & Planetary Science* 55, 1257–1280. <https://doi.org/10.1111/maps.13383>
- VACHER, L.G., PIANI, L., RIGAUDIER, T., THOMASSIN, D., FLORIN, G., PIRALLA, M., MARROCCHI, Y. (2020) Hydrogen in chondrites: Influence of parent body alteration and atmospheric contamination on primordial components. *Geochimica et Cosmochimica Acta* 281, 53–66. <https://doi.org/10.1016/j.gca.2020.05.007>
- WIELER, R., ANDERS, E., BAUR, H., LEWIS, R.S., SIGNER, P. (1991) Noble gases in “phase Q”: Closed-system etching of an Allende residue. *Geochimica et Cosmochimica Acta* 55, 1709–1722. [https://doi.org/10.1016/0016-7037\(91\)90141-Q](https://doi.org/10.1016/0016-7037(91)90141-Q)



Origin of radiogenic ^{129}Xe variations in carbonaceous chondrites

G. Avice, M.M.M. Meier, Y. Marrocchi

Supplementary Information

The Supplementary Information includes:

- Analytical Methods
- Cosmogenic and Radiogenic Contributions
- Tables S-1 and S-2
- Figures S-1 to S-5
- Supplementary Information References

Analytical Methods

Noble gases were released from bulk fragments of Tarda, Orgueil and Tagish Lake meteorites in two extraction steps using a heating laser diode ($\lambda=1064$ nm). The first extraction step used medium laser power (1 A). The final steps were done at high laser power (5 A) until complete melting of the sample was observed. Each extraction step lasted 2 min. After extraction, reactive gases were purified sequentially using three getters (one containing V-Cr-Fe pellets and two containing Ti sponge) operated at high temperature during 5 min (300 and 800 °C for the pellets and the Ti-sponge, respectively) and cooled down to room temperature during 10 min. After removal of reactive gases, noble gases were adsorbed during 15 min on a charcoal cooled down to 10 K by a cryopump. Noble gases were then sequentially released from the charcoal by heating the cryotrap with a resistance wire. Noble gases were exposed to a D100 Capacitorr[®] SAES getter for 15 min before being admitted in the Noblesse[®] noble gas mass spectrometer. Neon isotopes were detected in multi-collection mode using three electron multipliers. $^{40}\text{Ar}^+$, CO_2^+ signals were also measured between each neon integration cycles to correct for $^{40}\text{Ar}^{++}$ ($m = 20$) and CO_2^{++} ($m = 22$) interferences on neon signals. These corrections were applied by using the double ionisation ratios ($^{40}\text{Ar}^{++}/^{40}\text{Ar}^+=10.5\%$ and $\text{CO}_2^{++}/\text{CO}_2^+=1.2\%$). Argon isotopes were measured in multi-collection mode using a faraday cup for ^{40}Ar and electron multipliers for ^{38}Ar and ^{36}Ar . Krypton and xenon isotopes were measured in peak-jumping mode using an electron multiplier.

The sensitivity and the reproducibility of the instrument were determined by measuring known amounts of noble gases in aliquots taken from a standard bottle prepared from ambient air. Analytical blanks were measured repeatedly over the course the analytical session and were negligible: 2.9×10^{-14} cm³ STP of ^{22}Ne *i.e.* <0.2 % of the ^{22}Ne released during one extraction step, 1.01×10^{-11} cm³ STP of ^{36}Ar *i.e.* <2 % ^{36}Ar released during one extraction step, 7.49×10^{-14} cm³ STP of ^{84}Kr *i.e.* <1 % of the ^{84}Kr released during one extraction step and 3.65×10^{-15} cm³ STP of ^{130}Xe *i.e.* <1 % of

the ^{130}Xe released during one extraction step). All data have been corrected for blank contributions and mass discrimination of the instrument. Errors on isotope ratios include internal errors, external errors assessed by repeated measurements of standard aliquots and errors on the blank contribution.

Cosmogenic and Radiogenic Contributions

Presence and isolation of cosmogenic Ne

In all three meteorites analysed here, the cosmogenic component is resolvable only in Ne (it might be resolvable in He, too, which was not measured). All 12 samples show a slight excess of ^{21}Ne relative to the dominant trapped Ne component. The latter is likely a mixture between the planetary component phase Q (*e.g.*, Busemann *et al.*, 2000) and presolar components including P3, Ne-HL and Ne-E (*e.g.*, Ott, 2014). The observed ^{21}Ne -excesses are due to cosmogenic Ne (*i.e.* Ne produced by cosmic-ray-induced spallation of Mg, Si, Al), the concentration of which can be determined using a two- or three-component-deconvolution approach, provided the isotopic compositions of the end-members are known. Interestingly, three of the Tarda samples and both Tagish Lake samples (samples = total gas released in the 1A and 5A extractions) plot very close to a single line in the Ne-three-isotope diagram (Fig. 1), which can be extrapolated to $^{20}\text{Ne}/^{22}\text{Ne} \sim 7.5$ at $^{21}\text{Ne}/^{22}\text{Ne} \sim 0.03$. That value likely represents the isotopic composition of the characteristic mixture of presolar and planetary components in both Tarda and Tagish Lake. It is remarkable that the samples from both meteorites plot on the same line, with no discernible difference – this could suggest that both Tarda and Tagish Lake sample the same source material. A fourth Tarda sample plots slightly below that trend line, perhaps suggesting sample heterogeneity. On the other hand, the two Orgueil samples plot significantly above that line, indicating the additional presence of a ^{20}Ne -rich component, which could be, *e.g.*, implanted solar wind or a higher relative contribution of Ne-Q. Extrapolating the Tarda / Tagish Lake trend-line towards the cosmogenic end-member might potentially reveal its $^{22}\text{Ne}/^{21}\text{Ne}$ ratio (while the $^{20}\text{Ne}/^{22}\text{Ne}$ -ratio of cosmogenic Ne can be assumed to be constant at ~ 0.81 according to the model calculations of Leya and Masarik, 2009). The cosmogenic $^{22}\text{Ne}/^{21}\text{Ne}$ -ratio is often used to determine the production rate of cosmogenic ^{21}Ne (the “ $^{22}\text{Ne}/^{21}\text{Ne}$ - ^{21}Ne -method” of cosmic-ray exposure (CRE) age dating, *e.g.*, Leya and Masarik, 2009). For the same chemical composition, higher values of that ratio are associated with lower shielding in smaller meteoroids, while lower values are associated with higher shielding in larger meteoroids. The shielding (essentially, the amount of material between a target meteorite sample and the cosmic-ray source) determines the production rate of ^{21}Ne , which increases from the meteoroid surface towards the interior, reaches its maximum a few 10 cm below the surface, and eventually tails off towards zero deep inside a large meteoroid (see Fig. S-3). However, extrapolation of the Tarda/Tagish Lake trend-line to $^{20}\text{Ne}/^{22}\text{Ne} = 0.81$ yields a cosmogenic $^{22}\text{Ne}/^{21}\text{Ne}$ of ~ 1.0 , which is nominally below the expected range of 1.09-1.22 (Fig. S-3), but the associated uncertainties are likely to be large. Therefore, as is characteristic for primitive carbonaceous chondrites (*e.g.*, Krietsch *et al.*, 2021), the trapped Ne component is so dominant in all three meteorites that the $^{22}\text{Ne}/^{21}\text{Ne}$ -ratio of the cosmogenic end-member cannot be reliably determined. Therefore, we will only be able to give a very rough estimate of the shielding (based on estimated meteoroid sizes), the ^{21}Ne production rates and thus the CRE ages of the three meteorites.



Meteoroid sizes and cosmogenic ^{21}Ne production rates

As shown in Figure S-3, the expected $^{22}\text{Ne}/^{21}\text{Ne}$ ratios and ^{21}Ne production rates (based on the carbonaceous chondrite model from Leya and Masarik, 2009, with target chemistry changed to reflect the composition of Tarda / Tagish Lake, see Marrocchi *et al.*, 2021) show some clear variability as a function of shielding position (the surface is located at the top left end of the lines shown in Fig. S-3), but also as a function of overall meteoroid size (note that all given radii have been recalculated for a density of 1.5 g cm^{-3} typical for Tarda / Tagish Lake, Brown *et al.*, 2000). Meteoroid size has only been reliably determined for Tagish Lake, where it was given as 2-3 m in radius (Brown *et al.*, 2000; blue lines in Fig. S-3). Only about 10 kg of material were found on the surface within a $16 \text{ km} \times 3 \text{ km}$ strewn field (corresponding to 0.005 % - 0.02 % of the initial mass). For Orgueil, which was reported as a very bright fireball (visible over several 100 km, similar to Tagish Lake), about 14 kg were delivered to the surface within a $20 \text{ km} \times 4 \text{ km}$ strewn field (Gounelle and Zolensky, 2014). Given very similar physical properties (density, porosity, low coherence, *etc.*), we can probably assume that this indicates that the Orgueil meteoroid was at least as large as the Tagish Lake meteoroid. For Tarda, only about 4 kg were found on the surface, the strewn field is only about 3 km long, and the fireball was not exceptionally bright. This suggests, to first order, that the Tarda meteoroid was smaller than the Orgueil or Tagish Lake ones, although given the similar masses found, it seems very unlikely that it would be several orders of magnitude smaller (typical ablation rates of 27-99.9 % with a median of 85 %, determined for mostly small ordinary chondrites with initial masses of 10-1000 kg (Bhandari *et al.*, 1980), are not directly applicable to these friable and - certainly in the case of Tagish Lake and Orgueil - metre-sized, multi-ton meteoroids). Still, we cannot technically exclude the smallest meteoroid sizes at this point, and determine a ^{21}Ne production rate range of $(0.11-0.28) \times 10^{-8} \text{ cm}^3 \text{ STP g}^{-1} \text{ Ma}^{-1}$ for Tarda. For Tagish Lake, the known radius of the Tagish Lake meteoroid allows for a slightly more constrained ^{21}Ne production rate range, of $(0.13-0.23) \times 10^{-8} \text{ cm}^3 \text{ STP g}^{-1} \text{ Ma}^{-1}$. For Orgueil, we use the basic carbonaceous chondrite model by Leya and Masarik (2009), which was calculated for CI-chondrite chemistry (not shown in Fig. S-3) and adopt a slightly lower ^{21}Ne production rate range of $(0.11-0.20) \times 10^{-8} \text{ cm}^3 \text{ STP g}^{-1} \text{ Ma}^{-1}$.

Cosmic-ray exposure ages

Cosmic-ray exposure ages (or age ranges) are calculated by dividing the cosmogenic ^{21}Ne concentration by the production rate, or in this case, by the production rate range. The cosmogenic concentrations are consistent (within uncertainties) between the two samples of Orgueil, and the two samples of Tagish Lake. Within Tarda, we found two different sets of concentrations among the four samples, with the lower concentration set (Tarda B and D) having about 50 % of the cosmogenic ^{21}Ne compared to the higher concentration set (Tarda A and C). Since the concentration of trapped gases is also lower in the lower concentration set, it is possible that both Tarda B and D lost some of their Ne, in a similar fashion. The most straightforward explanation is that these samples contained fusion crust (and were thus partially degassed), the presence of which is difficult to recognise under the microscope due to the dull-black coloration of the interior of Tarda fragments. However, differences due to a different target chemistry (*e.g.*, carbonates or anorthite) cannot be fully excluded. At this point, we exclude the two samples from the CRE age determination (see Table S-2). The CRE ages are given in Table S-2 – note that since we use the full range of possible production rates, the true CRE ages must be somewhere in-between the $T21_{\text{low}}$ and $T21_{\text{high}}$ ages given.

Radiogenic Ar

The $^{40}\text{Ar}/^{36}\text{Ar}$ ratios in all measured samples are clearly non-terrestrial at ~9-14. Although the measured $^{38}\text{Ar}/^{36}\text{Ar}$ ratios are compatible with both extra-terrestrial trapped or atmospheric ratios, and thus a small contribution from (adsorbed)



atmospheric Ar cannot be conclusively excluded, we can at least determine upper limits to the K-Ar radiogenic gas retention (RGR) ages of the samples by assuming all of their ^{40}Ar is radiogenic. We adopt K concentrations of 660, 650 and 550 ppm for Tarda, Tagish Lake and Orgueil, respectively (Brown *et al.*, 2000; Marrocchi *et al.*, 2021). This results in the K-Ar (upper limit) ages given in the R40 column in Table S-2. The values are given without uncertainty since the inter-sample variation provides a better estimate of the reproducibility of the RGR age than the precision to which the ^{40}Ar was measured.



Supplementary Tables

Table S-1 Elemental abundances (in units of $\text{cm}^3 \text{STP g}^{-1}$) and isotopic compositions of Ne, Ar, Kr & Xe extracted from Tarda, Tagish Lake and Orgueil samples analysed in this study. Heating steps 1 & 2 correspond to laser power of 1 and 5 A, respectively. Uncertainties correspond to 1σ .

Table S-1 is available to download (Excel) from the online version of the article at <https://doi.org/10.7185/geochemlet.2228>

Table S-2 Cosmogenic concentrations, production rates, exposure ages. $^{21}\text{Ne}_{\text{cos}}$: Concentration of cosmic-ray produced ^{21}Ne , in units of $10^{-8} \text{cm}^3 \text{STP g}^{-1}$. P21: Estimated likely range of the production rate of ^{21}Ne , in units of $10^{-8} \text{cm}^3 \text{STP g}^{-1} \text{Ma}^{-1}$. T21: Cosmic-ray exposure age, low- and high-end estimate, in Ma. R40: Upper limit on the K-Ar RGR age, in Ga. *Two samples from Tarda did not release as much Ne as the others, probably because they contained fusion crust (see main text). 1σ uncertainties.

Sample	$^{21}\text{Ne}_{\text{cos}}$	P21	T21 _{low}	T21 _{high}	R40
Tarda A	1.40±0.34	0.13-0.28	5.0±1.2	12.7±3.0	2.59
Tarda B	0.60±0.15*	0.13-0.28	-	-	2.68
Tarda C	1.24±0.31	0.13-0.28	4.4±1.1	11.3±2.8	2.61
Tarda D	0.55±0.14*	0.13-0.28	-	-	2.44
Tagish Lake A	1.16±0.29	0.13-0.23	5.0±1.3	8.9±2.2	2.84
Tagish Lake B	0.99±0.25	0.13-0.23	4.3±1.1	7.6±1.9	2.05
Orgueil A	1.22±0.32	0.11-0.20	6.1±1.6	11.1±2.9	2.69
Orgueil B	1.21±0.32	0.11-0.20	6.1±1.6	11.0±2.9	2.22



Supplementary Figures

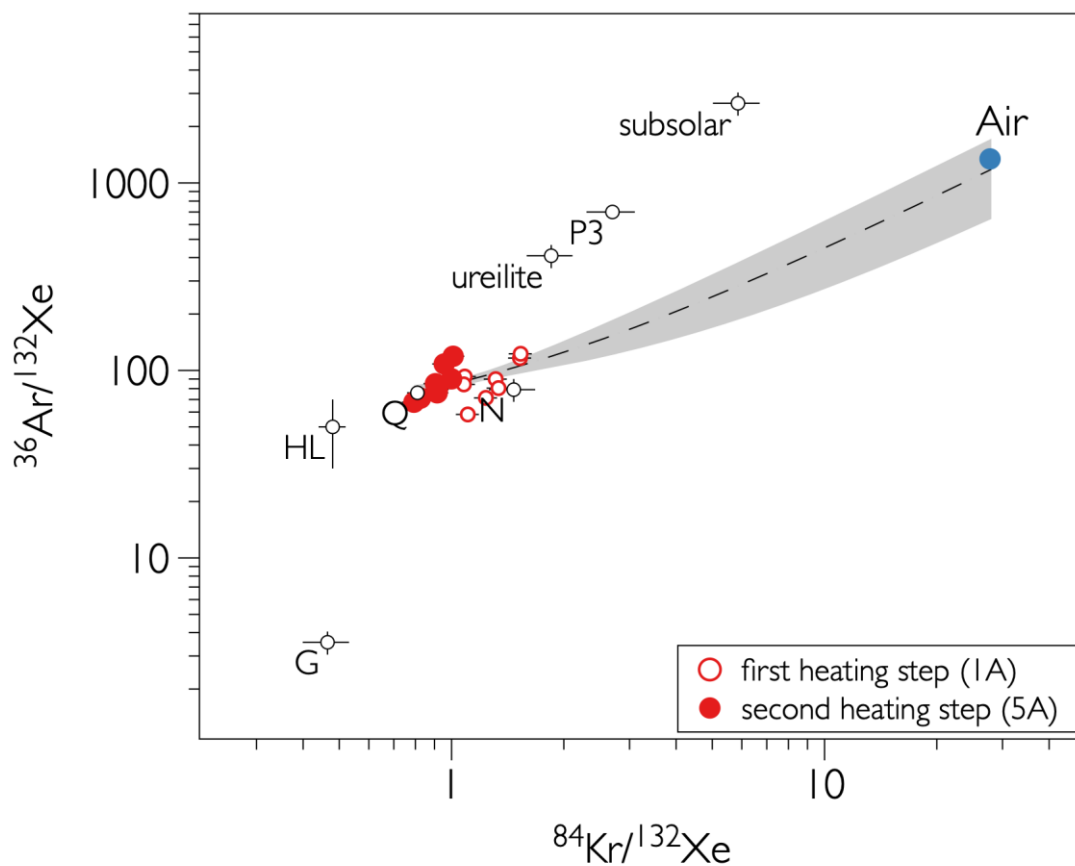


Figure S-1 Elemental abundance ratios for samples measured in this study. For clarity, samples are not identified and only first and second heating steps are represented. Low temperature heating steps plot toward the Air component. The dashed line and grey area ($\pm 1\sigma$) correspond to a linear fit through the entire dataset. High temperature heating steps plot close to the Q component. Figure adapted from Ott (2002). See also Ott (2002) for references for the elemental ratios of primordial components in the Solar System.

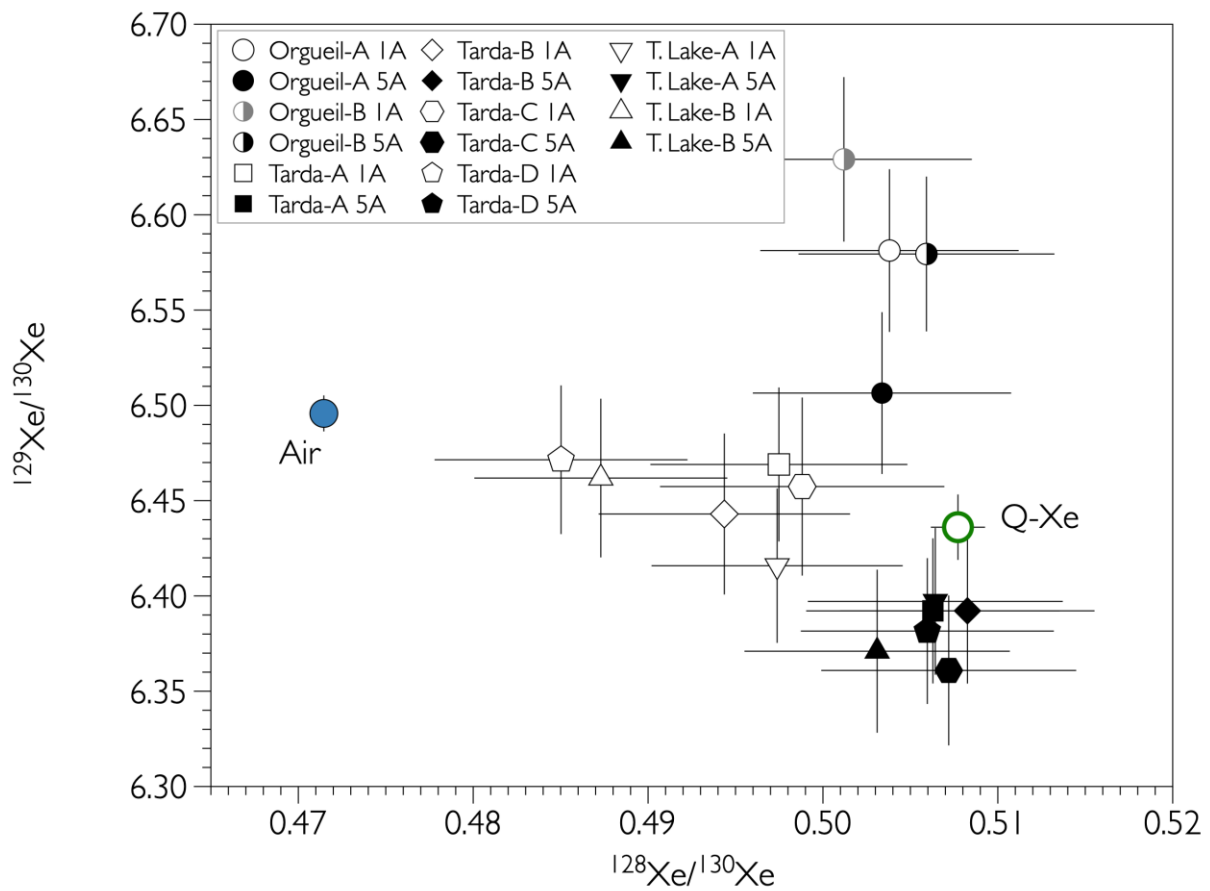


Figure S-2 Three-isotope plot of xenon. Low temperature heating steps show a tendency toward atmospheric xenon (Air, Ozima and Podosek, 2002). Xenon released during high temperature heating steps of Tarda and Tagish Lake samples has a $^{129}\text{Xe}/^{130}\text{Xe}$ ratio systematically lower than the Q component (Busemann *et al.*, 2000). Errors are at 1σ .

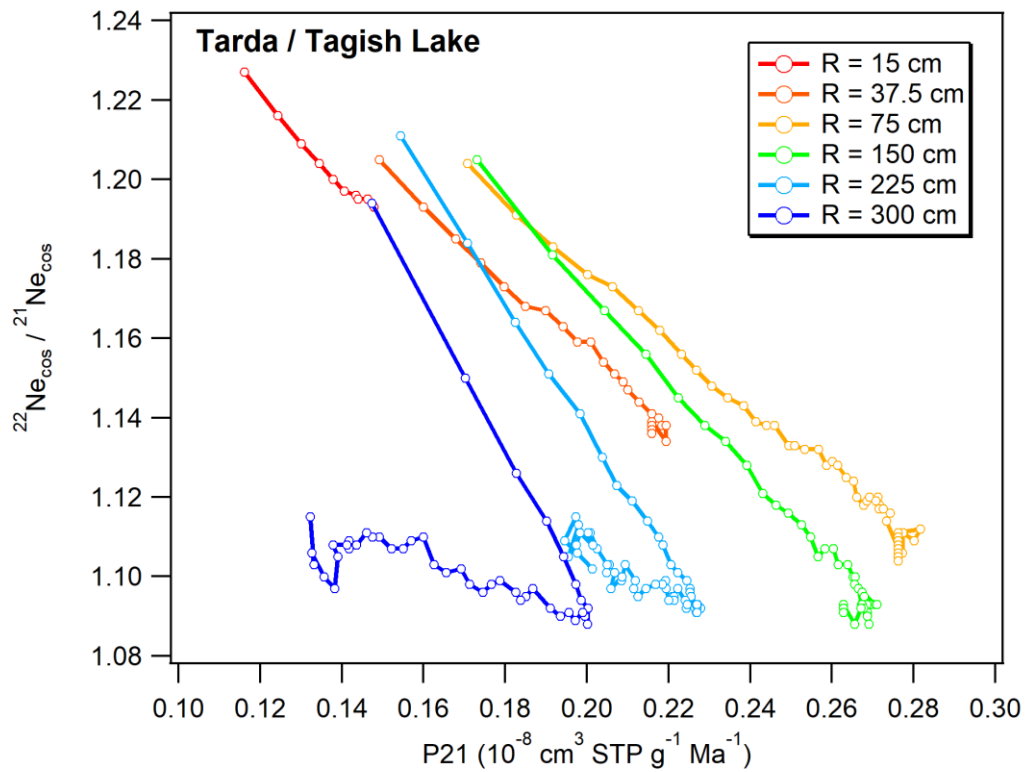


Figure S-3 Cosmogenic $^{22}\text{Ne}/^{21}\text{Ne}$ ratio and P21 for different sizes of meteoroids (radii given in the legend) with a Tarda / Tagish Lake-like target chemistry

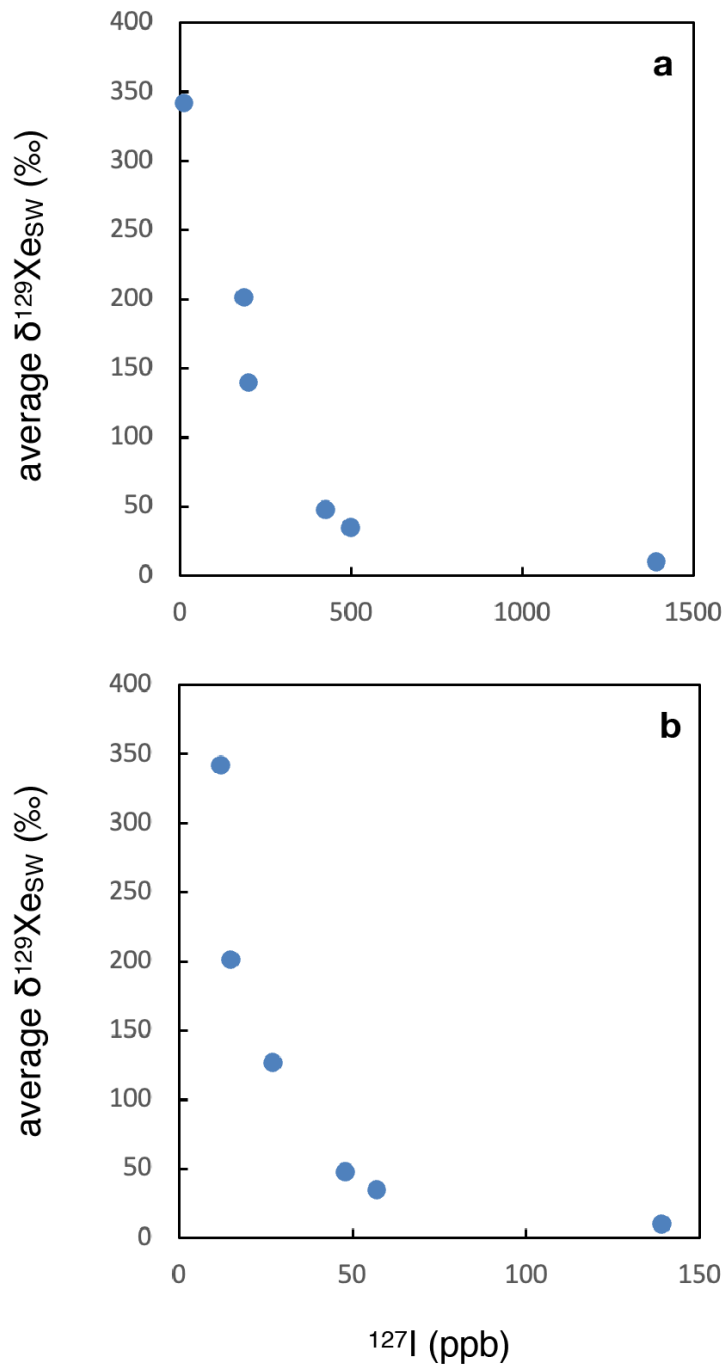


Figure S-4 Variations of excesses of ^{129}Xe relative to Solar Wind Xe (see also Fig. 3a) for two sets of estimates of the iodine content (^{127}I in ppb) of meteorites. **(a)** Iodine estimates obtained by the neutron activation method (data are from Dreibus *et al.* (1979) and Day *et al.* (2016)). **(b)** Iodine estimates obtained via the Ar-Ar method (data taken from Clay *et al.* (2017)).

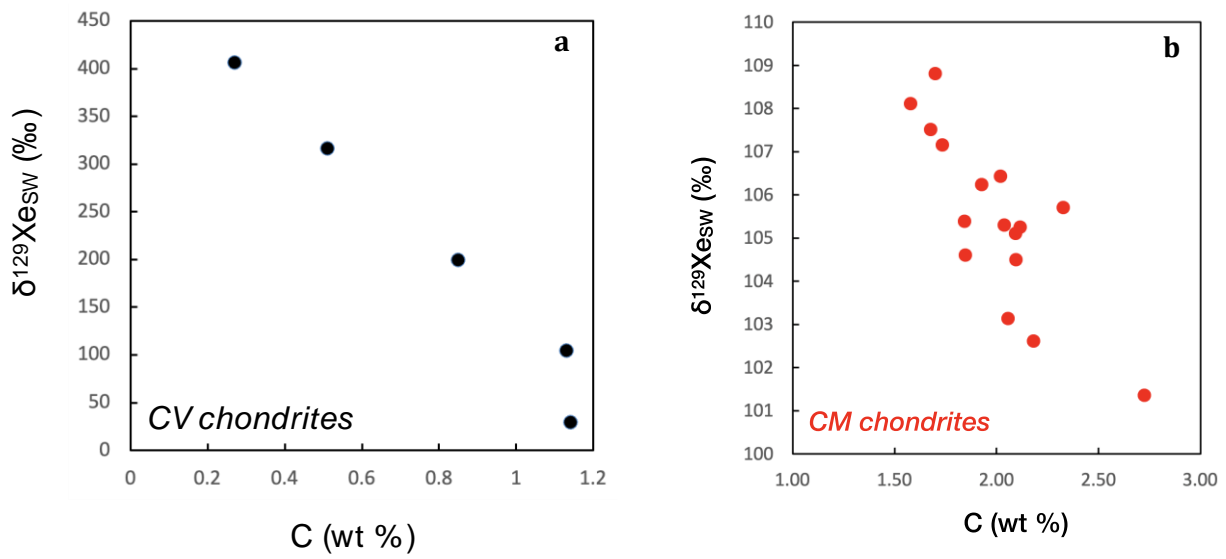


Figure S-5 Variations of excesses of ^{129}Xe relative to Solar Wind Xe within two meteorite groups. **(a)** CV chondrites, **(b)** CM chondrites. Data are from Alexander *et al.* (2012) and Kerridge (1985). Noble gas data are from Mazor (1970).

Supplementary Information References

- Alexander, C.M.O.'D, Bowden, R., Fogel, M.L., Howard, K.T., Herd, C.D.K., Nittler, L.R. (2012) The Provenances of Asteroids, and Their Contributions to the Volatile Inventories of the Terrestrial Planets. *Science* 337, 721–723. <https://doi.org/10.1126/science.1223474>
- Bhandari, N., Lal, D., Rajan, R.S., Arnold, J.R., Marti, K., Moore, C.B. (1980) Atmospheric ablation in meteorites: A study based on cosmic ray tracks and neon isotopes. *Nuclear Tracks* 4, 213–262. [https://doi.org/10.1016/0191-278X\(80\)90037-2](https://doi.org/10.1016/0191-278X(80)90037-2)
- Brown, P.G., Hildebrand, A.R., Zolensky, M.E., Grady, M., Clayton, R.N., Mayeda, T.K., Tagliaferri, E., Spalding, R., MacRae, N.D., Hoffman, E.L., Mittlefehldt, D.W., Wacker, J.F., Bird, J.A., Campbell, M.D., Carpenter, R., Gingerich, H., Glatiotis, M., Greiner, E., Mazur, M.J., McCausland, P.J.A., Plotkin, H., Mazur, T.R. (2000) The Fall, Recovery, Orbit, and Composition of the Tagish Lake Meteorite: A New Type of Carbonaceous Chondrite. *Science* 290, 320–325. <https://doi.org/10.1126/science.290.5490.320>
- Busemann, H., Baur, H., Wieler, R. (2000) Primordial noble gases in “phase Q” in carbonaceous and ordinary chondrites studied by closed-system stepped etching. *Meteoritics and Planetary Science* 35, 949–973. <https://doi.org/10.1111/j.1945-5100.2000.tb01485.x>
- Clay, P.L., Burgess, R., Busemann, H., Ruzié-Hamilton, L., Joachim, B., Day, J.M.D., Ballentine, C.J. (2017) Halogens in chondritic meteorites and terrestrial accretion. *Nature* 551, 614–618. <https://doi.org/10.1038/nature24625>
- Day, J.M.D., Brandon, A.D., Walker, R.J. (2016) Highly siderophile elements in Earth, Mars, the Moon & Asteroids. *Reviews in Mineralogy and Geochemistry* 81, 161–238. <https://doi.org/10.2138/rmg.2016.81.04>
- Dreibus, G., Spettel, B., Wänke, H. (1979) Halogens in meteorites and their primordial abundances. *Physics and Chemistry of the Earth* 11, 33–38. [https://doi.org/10.1016/0079-1946\(79\)90005-3](https://doi.org/10.1016/0079-1946(79)90005-3)
- Gounelle, M., Zolensky, M.E. (2014) The Orgueil meteorite: 150 years of history. *Meteoritics and Planetary Science* 49, 1769–1794. <https://doi.org/10.1111/maps.12351>
- Kerridge, J.F. (1985) Carbon, hydrogen and nitrogen in carbonaceous chondrites: abundances and isotopic compositions in bulk samples. *Geochimica et Cosmochimica Acta* 49, 1707–1714. [https://doi.org/10.1016/0016-7037\(85\)90141-3](https://doi.org/10.1016/0016-7037(85)90141-3)
- Krietsch, D., Busemann, H., Riebe, M.E.I., King, A.J., Alexander, C.M.O., Maden, C. (2021) Noble gases in CM carbonaceous chondrites: Effect of parent body aqueous and thermal alteration and cosmic ray exposure ages. *Geochimica et Cosmochimica Acta* 310, 240–280. <https://doi.org/10.1016/j.gca.2021.05.050>
- Leya, I., Masarik, J. (2009) Cosmogenic nuclides in stony meteorites revisited. *Meteoritics and Planetary Science* 44, 1061–1086. <https://doi.org/10.1111/j.1945-5100.2009.tb00788.x>
- Marrocchi, Y., Avice, G., Barrat, J.-A. (2021) The Tarda Meteorite: A Window into the Formation of D-type Asteroids. *The Astrophysical Journal Letters* 913, 8. <https://doi.org/10.3847/2041-8213/abfaa3>
- Mazor, E., Heymann, D., Anders, E. (1970) Noble gases in carbonaceous chondrites. *Geochimica et Cosmochimica Acta* 34, 781–824. [https://doi.org/10.1016/0016-7037\(70\)90031-1](https://doi.org/10.1016/0016-7037(70)90031-1)
- Ott, U. (2002) Noble Gases in Meteorites - Trapped Components. *Reviews in Mineralogy and Geochemistry* 47, 71–100. <https://doi.org/10.2138/rmg.2002.47.3>
- Ott, U. (2014) Planetary and pre-solar noble gases in meteorites. *Chemie der Erde - Geochemistry* 74, 519–544. <https://doi.org/10.1016/j.chemer.2014.01.003>



Ozima, M., Podosek, F.A. (2002) Noble Gas Geochemistry. Cambridge University Press, Cambridge.

